Civil and Environmental Engineering
Vol. 20, Issue 1, 86-97, DOI: 10.2478/cee-2024-0008

TENSILE FORCES BEHAVIOR ON LONGITUDINAL REINFORCEMENT AND CFRP STRIPS ON CIRCULAR HOLLOW REINFORCED CONCRETE COLUMNS

Sri Hartati DEWI[1,2,*], Rendy THAMRIN[1], Sabril HARIS[1], Febi Putri YASTARI[1]

[1] Department of Civil Engineering, Andalas University, Padang, Indonesia.
[2] Department of Civil Engineering, Islamic University of Riau, Pekanbaru, Indonesia.
[*] corresponding author: srihartatidewi@eng.uir.ac.id

Abstract

Currently, there is not much research on strengthening structural elements with hollows. This manuscript presents the test results from twelve circular reinforced concrete column specimens strengthened with CFRP strips. This study focuses on the strain behavior of longitudinal reinforcement and CFRP strips due to high shear force intensity. Hollows in the cross-section are used to see the effect of voids on the column strain distribution. Nine specimens have a hollow cross-section with hollow diameters of 1.5", 2.5", and 3.5" for each of the three specimens. Meanwhile, the other three specimens have a solid cross-section. All specimens do not use stirrups to determine the contribution of concrete and CFRP strips to resist shear. Strain gauges are placed in certain positions to read the strain on the longitudinal reinforcement and CFRP strips. The test results are in the form of tensile forces and are then analyzed to obtain the movement pattern of tensile forces in the longitudinal reinforcement and CFRP strips. Numerical analysis using a fiber element model is used to obtain the strain in each reinforcement layer. The numerical analysis results were then compared with the test results and showed close results. Then, an equation for calculating the tensile force in CFRP strips is proposed. The proposed equation approximates the test results with an accuracy level of 90%.

Keywords:

Reinforced concrete;
Circular cross-section;
Hollow;
Shear strength;
CFRP strips.

1 Introduction

Diagonal cracks cause changes in the distribution of tensile forces in the longitudinal reinforcement and stirrups, particularly in the beam's shear span and support area [1]. CFRP sheets are widely used to strengthen structural elements to resist shear forces [2], [3]. Knowing the tensile force on the CFRP strip due to diagonal cracking is essential to avoid sudden failure due to CFRP rupture. Thamrin [4] proposed a model to calculate the tensile force in steel stirrups of reinforced concrete beams. However, no one has submitted an equation to calculate the tensile force on CFRP strips.

The circular cross-section was chosen in this study due to some reasons. Circular reinforced concrete has strong characteristics in all directions to withstand horizontal loads [5], [6]. Columns with circular cross-sections have a more uniform internal stress distribution than square or rectangular columns. Hence, circular cross-sections are also preferred to reduce stress concentrations [7]. These hollows are usually used to install pipes for electricity, rainwater or wastewater, and pipelines [8]. Hollow sections also reduce the column's material and self-weight, resulting in a more efficient construction system [9], [10]. However, the presence of a hole reduces the area and shear strength. Lately, the effect of the stirrup type on the shear strength of reinforced concrete specimens with solid circular cross-sections was studied in another reference [11]. This reference reported that the flexural capacity of specimens with closed spiral stirrups and hoops was almost the same, but the ductility of spiral hoops was slightly higher.

Shear failure is a sudden collapse that must be anticipated because it is extremely dangerous due to its brittle and sudden occurrence. This premature failure is typically caused by insufficient cross-sectional area and shear reinforcement to withstand shear, as well as other factors that reduce shear capacity. [12], [13], [14], and [15]. Due to changes made to the rules of the current seismic code, buildings built prior to the new regulation now require an assessment of their seismic resistance. Following revisions in seismic code rules, weakening structural parts due to hollows will increase the possibility of a choice to retrofit the structure. This circumstance needs structural engineers with extensive experience and knowledge in structural strengthening [16]. Carbon fiber-reinforced polymer (CFRP) sheet has recently gained popularity as a strengthening material and is more common in concrete structural repair and retrofitting. FRP has various advantages, including high tensile strength, quick transport, and site installation due to its lightweight and corrosion resistance [2] [17]. Lignola GP [18] reported that FRP jacketing could increase ultimate load and ductility significantly in the case of hollow cross sections and increase the seismic capacity by about 15%. One is easy to install and does not require heavy equipment. Wang et al. [19] investigated 11 CFRP-reinforced concrete columns. They discovered that the number of layers of externally wrapped CFRP sheets had minimal effect on the degradation of the effective and unloading stiffnesses of the concrete columns.

Despite numerous studies on applying FRP materials, information on the application of CFRP on hollow circular cross-sections to strengthen against shear forces remains limited. Therefore, in this study, the behavior of tensile forces on CFRP strips is discussed, and an equation is proposed to calculate these tensile forces. The experimental study was carried out using twelve circular cross-section specimens strengthened with CFRP strips consisting of three solid specimens, three 1.5" hollow specimens, three 2.5" hollow specimens, and three 3.5" hollow specimens. This study used CFRP strips with the wrapping installation method according to ACI-440.2R-17 [20] code.

2 Experimental Study

Tests were carried out on twelve reinforced concrete columns with a circular cross-section, a diameter of 250 mm, and a length of 2300 mm. The longitudinal reinforcement has diameters of 13 mm, 16 mm, and 19 mm, while the stirrup has a diameter of 10 mm with a modulus of elasticity of 200 GPa. Specimens were cast using ready-mix concrete ordered from a concrete supplier. Concrete's compressive strength was tested at 28 days using a standard test for the compressive strength of cylinder specimens and was found to be 40 MPa. CFRP strips with a thickness of 1 mm and a modulus of elasticity of 230 GPa are supported by Fyfe Fiberwrap Indonesia. The CFRP strips are installed in two layers with a width of 50 mm each and with a spacing between CFRP strips of 100 mm. Table 1 shows the material properties of the CFRP, steel bar, and concrete used in this study. The hollow diameters were 38.1 mm, 63.5 mm, and 88.9 mm for each specimen with hollow.

Table 1: Specification of Specimens.

Specimens							**Longitudinal reinforcement**			**CFRP Sheets**			
Code	***fc'***	***D_c***	***d***	***t***	***bw***	***a/d***	***ϕ_b***	***N***	***f_y***	***tf***	***wf***	***Ef***	***ffe***
	[MPa]	**[mm]**	**[mm]**	**[mm]**	**[mm]**		**[mm]**		**[MPa]**	**[mm]**	**[mm]**	**[MPa]**	**[MPa]**
Data from this study													
SR-1							13		427				
SR-2	40	250	200	0	250	2.50	16	3	492	1.0	50	230000	986
SR-3							19		416				
HR-2-1							13		436				
HR-2-2	30	250	200	93.3	187	2.50	16	3	471	1.0	50	230000	986
HR-2-3							19		492				
HR-3-1							13		436				
HR-3-2	30	250	200	86.9	174	2.50	16	3	471	1.0	50	230000	986
HR-3-3							19		492				
Thamrin et al. [15]													
HR-1-1							13		427				
HR-1-2	40	250	200	106	212	2.50	16	3	492	1.0	50	230000	986
HR-1-3							19		416				

Fig. 1 illustrates the schematic pictures of specimens with dimensions and details of reinforcement. The specimen was supported at a distance of 1500 mm by pin and rolled supports. The observed test span, covered with CFRP sheets, was 1000 mm long in the center zone of the specimen. The specimens were designed with sufficient bond length at the end to avoid bond failure [12].

The deflection and load were measured using three LVDTs and load cell, respectively. In addition, strain gauges were installed on longitudinal reinforcement, stirrups, and CFRP strips to collect the strain data. The strain gauge positions are shown in Fig. 1. SL represents the strain gauges installed on longitudinal reinforcement, SS represents the strain gauges installed on stirrups, and SF represents the strain gauges installed on CFRP strips. LVDTs, loadcell, and strain gauges were connected to the data logger to record data. The deflection data presented in this study is a deflection from an LVDT located in the midspan of the specimens. The cracks that occurred during the test were plotted to show the shape of the crack pattern of the specimen.

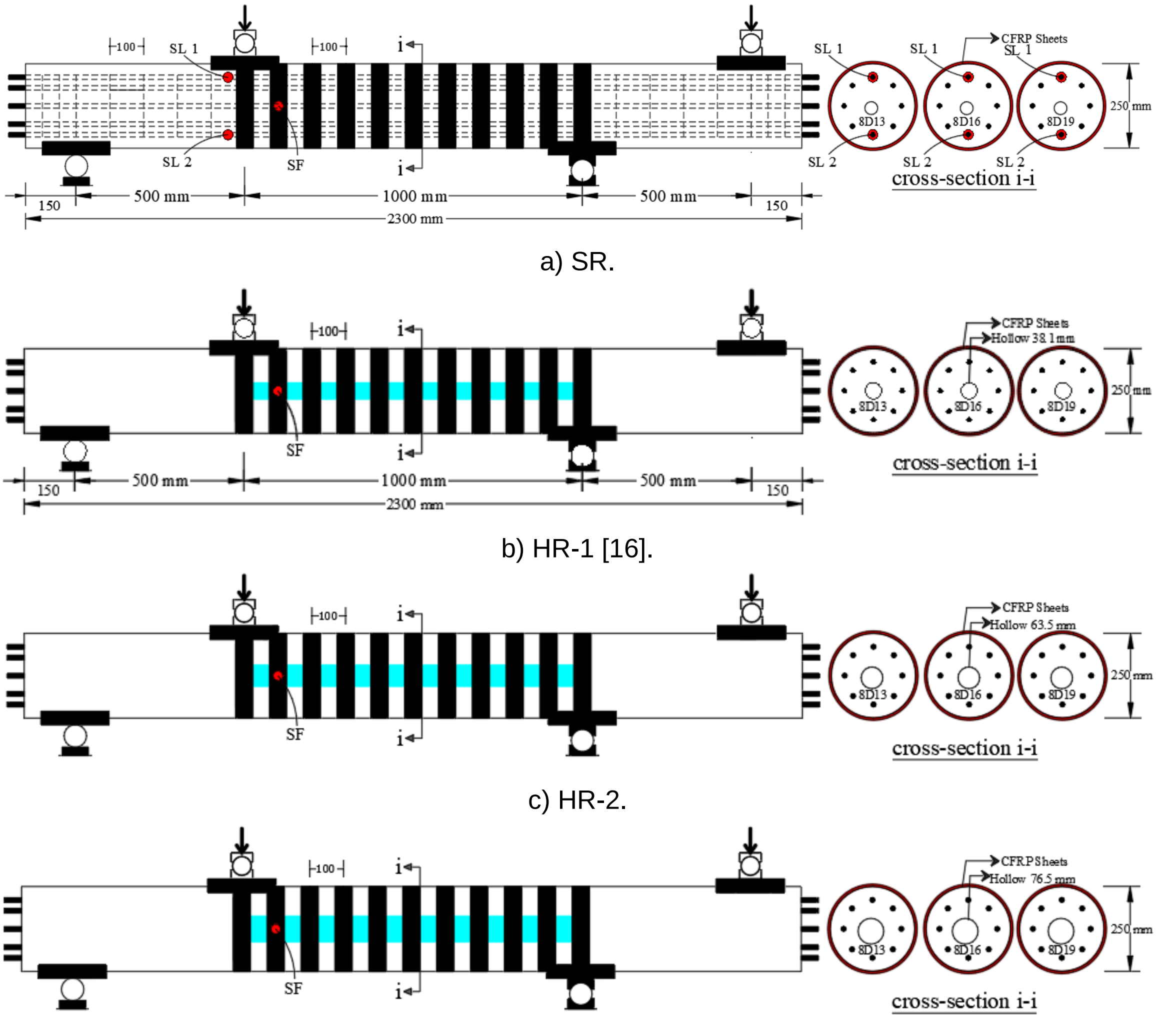

a) SR.

b) HR-1 [16].

c) HR-2.

d) HR-3.

Fig. 1: Cross-section and loading position of the specimens.

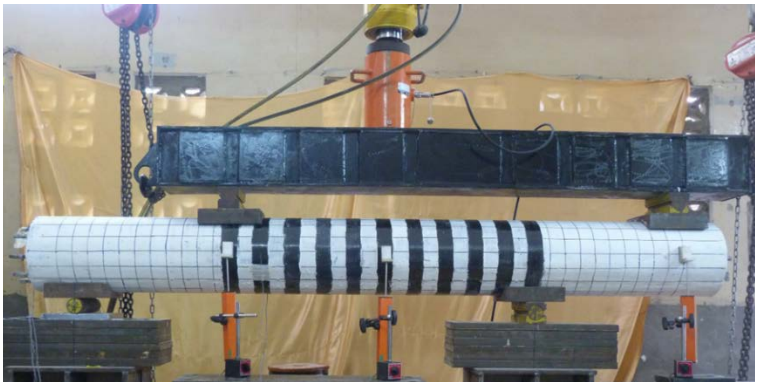

Fig. 2: Schematic pictures of the tested specimen and loading position.

An experimental study was carried out using an anti-symmetric four-point bending test method. The antisymmetric four-point bending test method produces a constant shear force and moment force that changes linearly along the observed zone [21], as desired in this study. Monotonic loading was applied in one direction with the load control method. The equipment used and test setup are shown in Fig. 2.

3 Analytical Study

The strain on longitudinal reinforcement of the specimens was determined using a computer program developed to obtain the moment-curvature relationship of a reinforced concrete cross-section. The computer program works with the fiber element model, where the concrete cross-section is divided into several layers in the vertical direction of the cross-section [22]. Some completed descriptions of the flexural analysis of reinforced concrete cross-sections using the fiber element model can be found in the references [23], [24], [25]. Nonlinear analysis of the fiber element model is carried out by the curvature incremental method and iterative procedure for each incremental step. This method divides the reinforced concrete section into several layers of thin elements. The longitudinal reinforcement is positioned parallel to the layers of the concrete elements, and the distance between each element is measured from the cross-section's top fiber (y_i). The area of each fiber element (A_i) can be calculated according to the element's geometric shape.

$$\varepsilon_i = \varepsilon_o - (\varphi y_i) \tag{1}$$

Where:
ε_i – strain in each layer,
y_i – distance from each element,
φ – the value of incremental curvature.

The current state of the stress at each strain level can further be calculated using the selected stress-strain relationship available in the computer program. The stress-strain law for concrete uses the Hognestad model found in [23], while the bilinear model is used for longitudinal reinforcement. The internal forces for each reinforcement and concrete layer can be calculated using each fiber element's stresses and area. The next step is checking whether the sum of internal forces satisfies the equilibrium condition. It uses an iterative procedure in which the equilibrium position of the neutral axis depth is successfully adjusted until the internal forces meet an equilibrium state for each value of incremental curvature. The moment (M) acted, and the appropriate curvature value for each incremental step can be obtained after each successful iteration level. The moment at each incremental curvature can be calculated using the equation as expressed in Equation (2):

$$M = \Sigma F_i y_i \tag{2}$$

where:
M – Moment,
y_i – distance from each element,
F_i – internal forces.

The same process is followed for the subsequent values of moment and curvature with uploading the incremental curvature. The integration procedure can be applied to calculate the deflection at each incremental step using the curvature values obtained at each step. The calculation process is completed when the value of maximum compressive strain of ε_{cm} = 0.003 is reached.

4 Theoretical Beam Capacities

The theoretical nominal shear strength (V_n) of the specimens is calculated using the available provisions based on the contribution of each component, contributions from concrete (V_c), and CFRP strips (V_{FRP}).

$$Vn = Vc + V_{FRP} \tag{3}$$

Where:
V_n – Nominal shear strength,
V_c – shear strength contributed by the concrete,
V_{FRP} – shear strength contributed by the CFRP.

The concrete contribution to the shear strength is calculated based on the equation provided by ACI 318-19 [26] as:

$$V_c = \left[0.66\lambda(\rho_w)^{1/3}\sqrt{f'c}\right] b_w d \tag{4}$$

$$\rho_w = \frac{A_S}{b_w d} \tag{5}$$

where:
V_c – the shear strength contributed by the concrete,
λ – a modification factor for concrete,
ρ_w – the ratio of tensile longitudinal reinforcement,
fc' – compressive strength of concrete,
b_w – the width of the reinforced concrete cross-section,
d – the effective depth,
A_s – the area of tensile longitudinal reinforcement.

Equation (4) is the equation for a rectangular cross-section. ACI-318-2019 [26] provides a new guideline for calculating the value of V_c for circular and hollow sections. This new regulation takes the effective height d as 0.8 of the cross-section diameter (D). For the hollow circular cross-section, the b_w value is twice the wall thickness. The reinforcement ratio in Equation (5) was calculated by dividing the nominal area of the tensile longitudinal reinforcement by the concrete's gross sectional area. Where: b_w is the width of reinforced concrete cross-section (for circular cross-section b_w is the diameter of the cross-section, and for hollow cross-section b_w is twice the wall thickness), d is the effective depth (for circular cross-section d is 0.8 times the diameter of the cross-section).

5 Results and Discussion

Experimental work has been carried out on twelve specimens, and the relationship between shear and deflection forces, distribution of strains and tensile forces in longitudinal reinforcement, and strain and tensile forces in CFRP strips will be discussed in this section.

• The shear force and deflection of the specimens

The test result shows that the specimen's first cracking load is around 20 kN. The first crack occurred in the region of the beam where the maximum moment occurred, specifically in the area under the left concentrated load and above the right support. After experiencing the first flexural crack, several flexural cracks appeared in the tensile region of the specimen. In the observed zone (between the left concentrated load and the right support), where large shear forces occur, the flexural crack develops into a diagonal crack. CFRP strips were proven to resist the shear forces well, and all specimens failed in the flexural mode indicated by crushing of concrete in the compression zone, as expected in this study.

The load-deflection curves of all specimens are plotted with analytical prediction and shown in Fig. 3. This figure simultaneously indicates the behavior of the specimens during loading until failure. All specimens prove the flexural failure indicated by the yielding of the longitudinal reinforcement followed by concrete crushing in the compression zone, as also obtained from the analysis results. The difference in the flexural capacity of the specimen is due to the variance in the ratio of the longitudinal reinforcement used in each specimen (with a diameter of 13 mm, 16 mm, and 19 mm). Fig. 3 shows that the specimen with a higher reinforcement ratio shows the highest flexural capacity but the lowest ductility value.

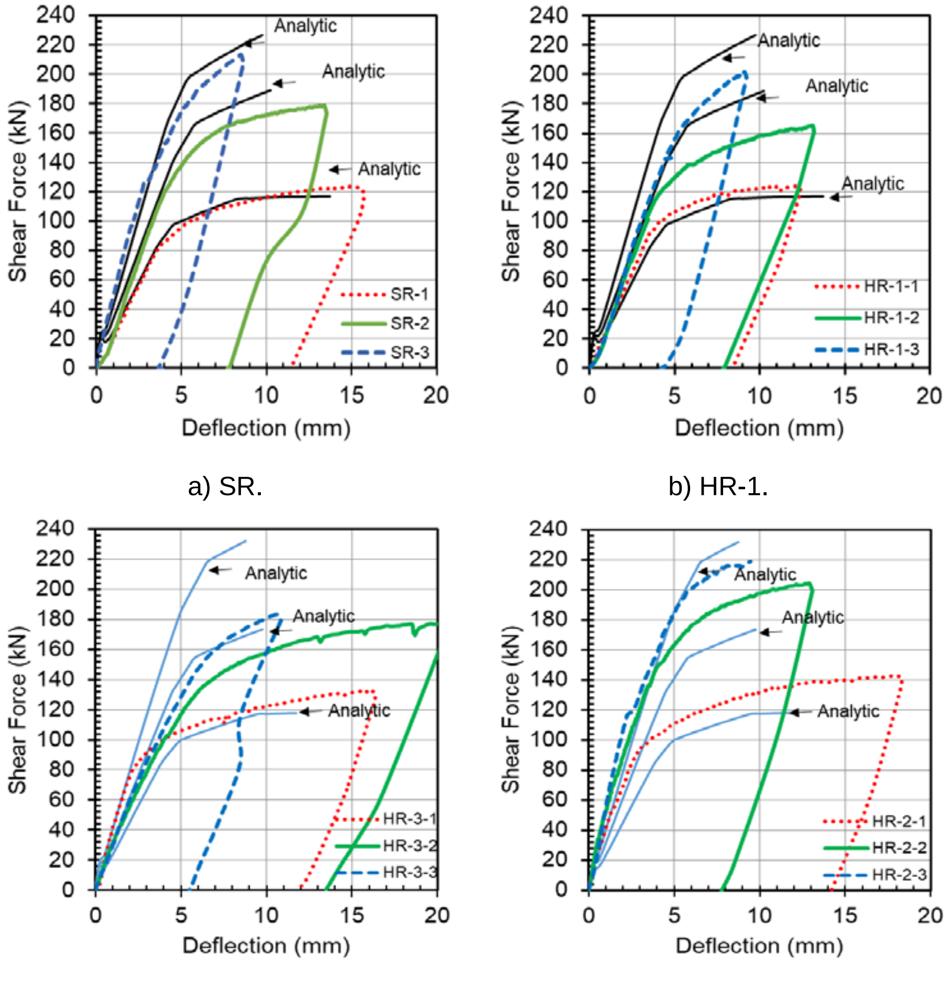

a) SR. b) HR-1.

c) HR-3. d) HR-2.

Fig. 3: Shear force vs deflection of specimens.

• The strain distribution and tensile forces on longitudinal reinforcement

Fig. 4 shows the stress distribution at failure for each specimen as determined by test results and analysis using a fiber element model. The *y*-axis notation represents the distance of each element to the top of the fiber section, while the *H* notation denotes the height of the cross-section. The longitudinal tension reinforcement of these two types of specimens is yielding (strain greater than 0.002), and the maximum compressive strain is close to 0.003. In comparison, the strain distributions from the results of analytical calculations are shown in Fig. 4 (m to o). The analysis results show an apparent sequence of strains in the longitudinal reinforcement where the strain decreases with increasing reinforcement ratio.

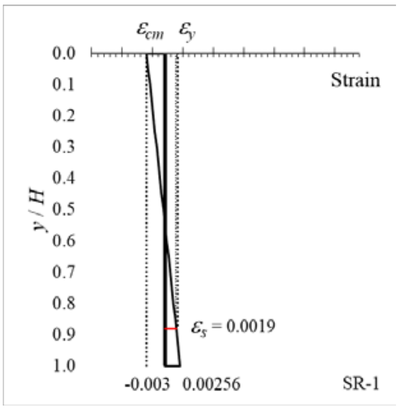

a) SR-1.

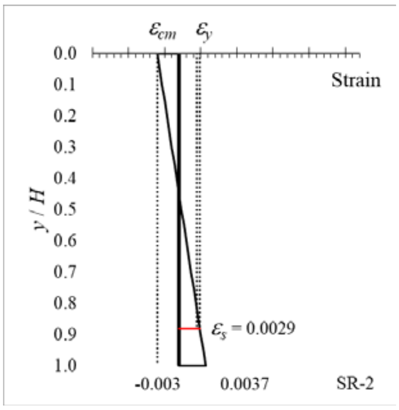

b) SR-2.

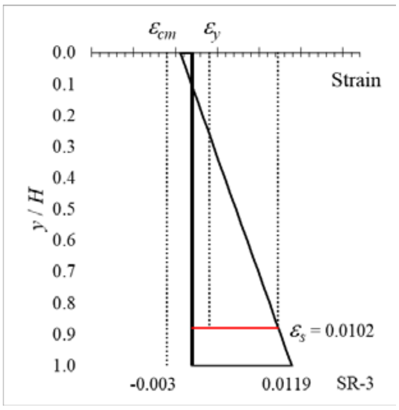

c) SR-3.

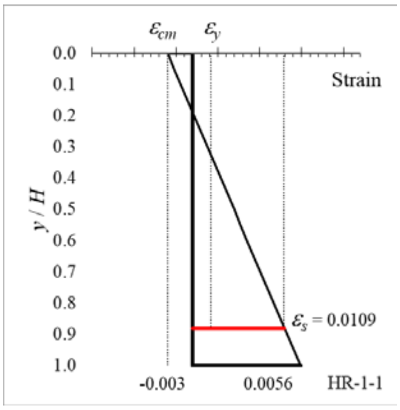

d) HR-1-1.

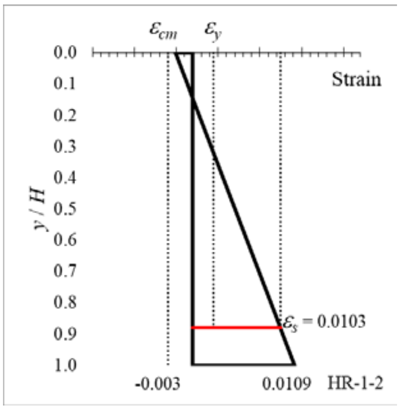

e) HR-1-2.

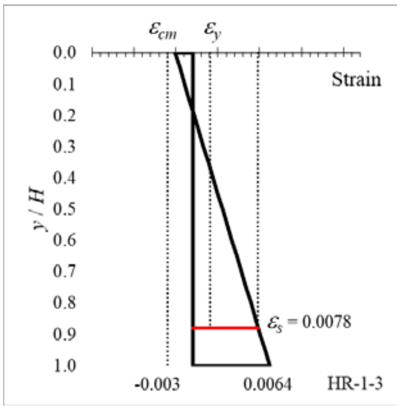

f) HR-1-3.

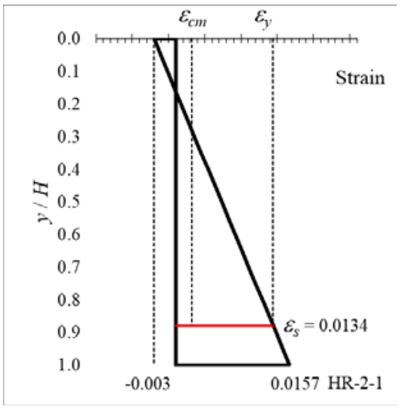

g) HR-2-1.

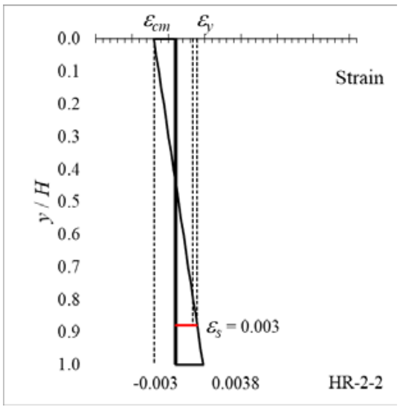

h) HR-2-2.

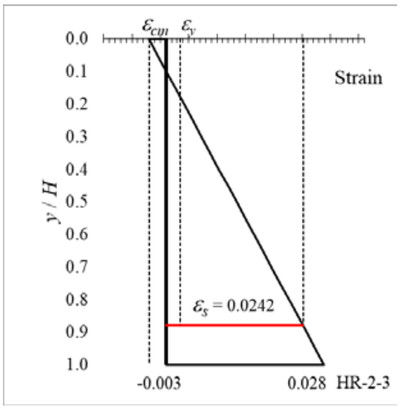

i) HR-2-3.

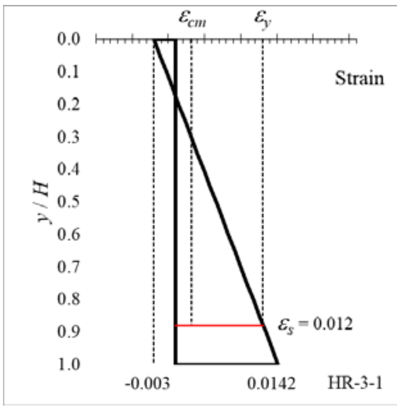

j) HR-3-1.

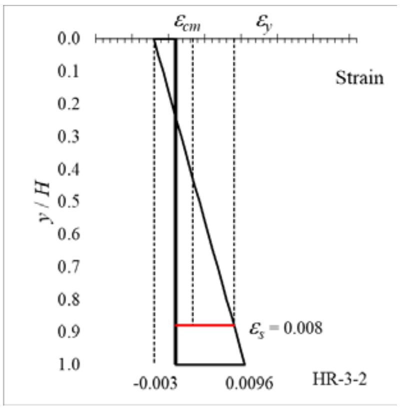

k) HR-3-1.

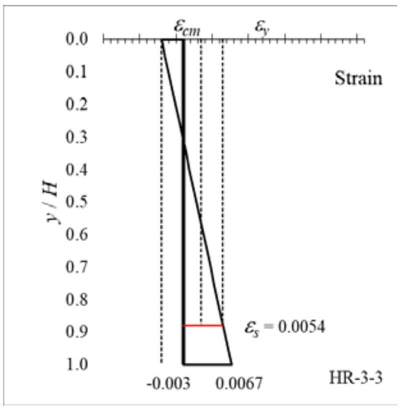

l) HR-3-1.

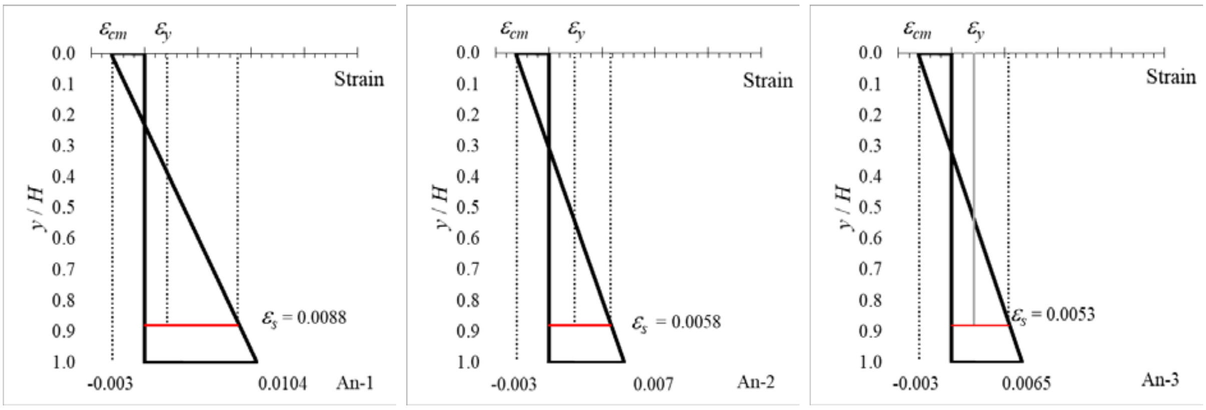

m) An-1. n) An-2. o) An-3.

Fig. 4: Strain distribution of the specimens.

The tensile forces in the longitudinal reinforcement obtained from the test and analysis results are shown in Fig. 5. As explained above, the strain gauge for reading the strain in the tensile reinforcement (SL2) is placed at the maximum bending moment. The growth of tensile force in the reinforcement changes significantly after the first crack occurs in the specimen. Next, the reinforcement's tensile force propagates towards the reinforcement's yield force, as shown in the analytical tensile force curve. Most experimental tensile force curves do not show the yielding of the reinforcement because the string gauge is damaged. A comparison between the analysis and the test results indicates quite good predictions.

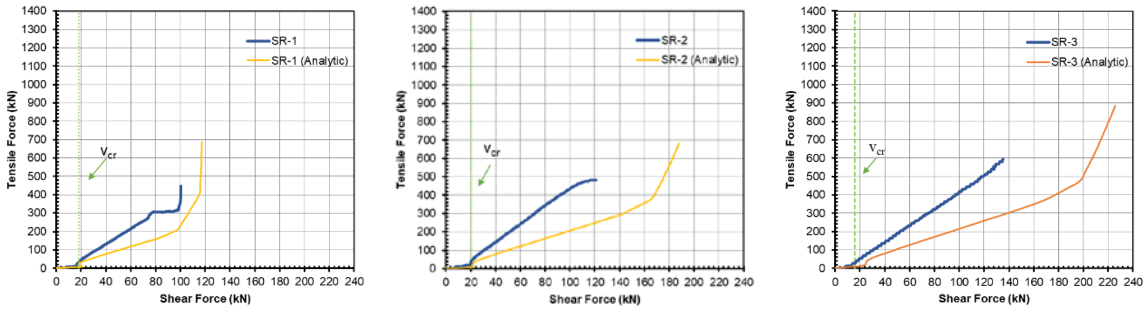

a) SR-1. b) SR-2. c) SR-3.

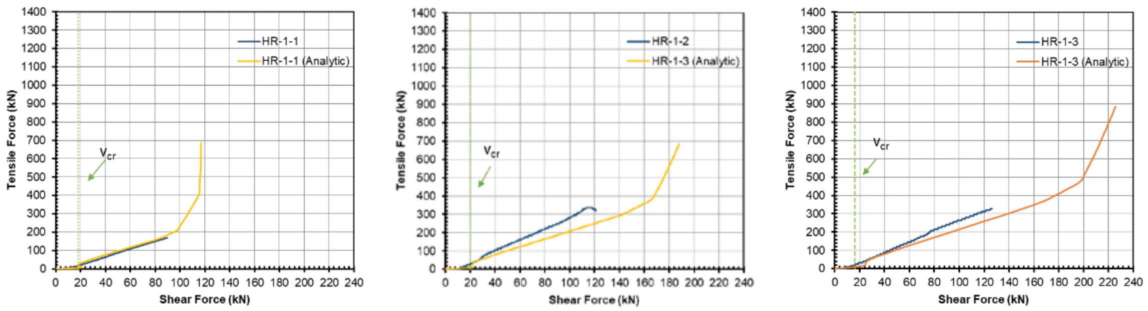

d) HR-1-1. e) HR-1-2. f) HR-1-3.

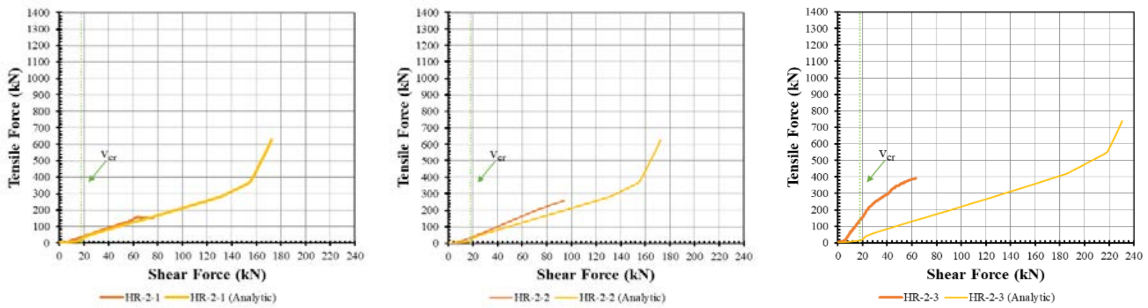

g) HR-2-1. h) HR-2-2. i) HR-2-3.

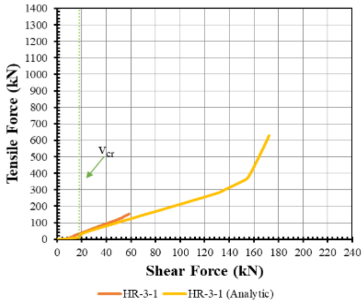

j) HR-3-1.

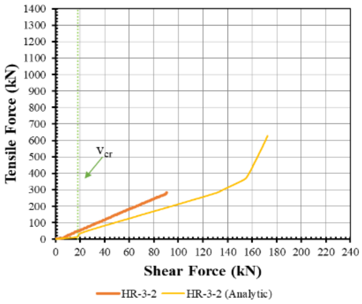

k) HR-3-2.

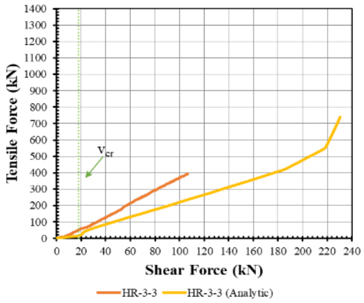

l) HR-3-3.

Fig. 5: Strain distribution of the specimens.

• Strain and tensile forces on CFRP strips

The strains on CFRP strips on the specimens obtained from the test results are plotted in Fig. 6. The curve shows that the strain values on the CFRP strips increase significantly after the shear load exceeds the value of V_c (concrete shear carrying capacity), which is identical to the occurrence of diagonal cracks. It means that the CFRP strips begin to carry significant tensile loads after the occurrence of diagonal cracking. This phenomenon is in accordance with what was found in the reference for steel stirrups [4]. After showing a significant increase in strain due to the occurrence of diagonal shear cracks, the strain value continues to increase in accordance with the increase in shear force. In this situation, only the CFRP strips resist the shear force because the shear load has exceeded the V_c value, and the specimen is not reinforced with stirrups.

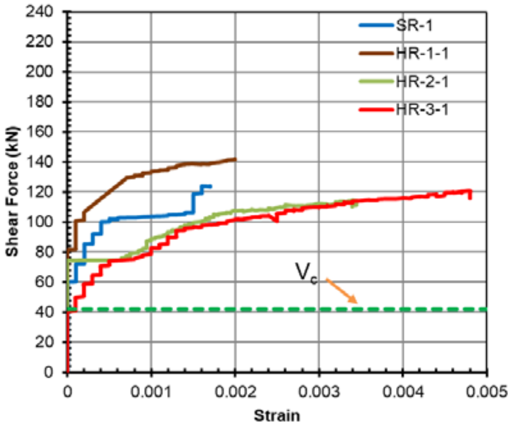

a) D13.

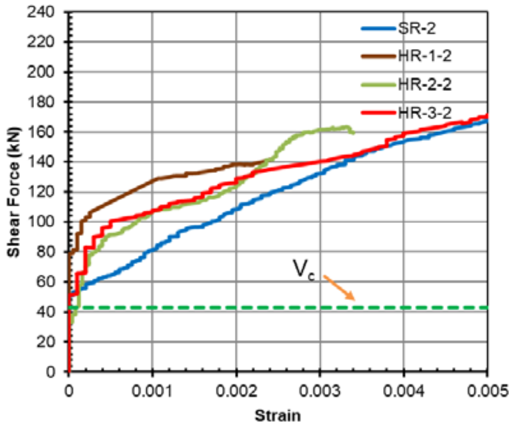

b) D16.

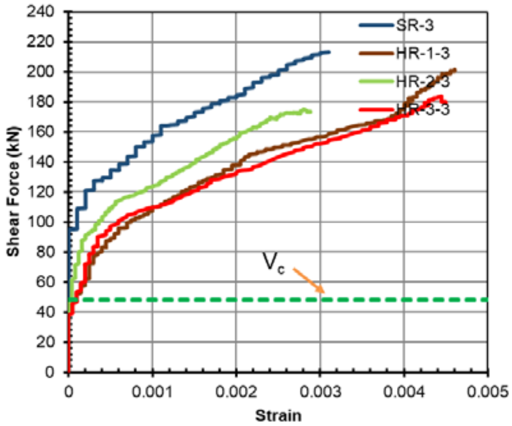

c) D19.

Fig. 6: Strain on CFRP strips.

Fig. 7 shows the curves of the tensile forces acting on the CFRP strips versus the shear forces for all specimens. The vertical dotted line indicates the value of the theoretical shear strength carried by concrete, V_c, which is calculated using Eq. 4, and the horizontal dashed line (T_{ffe}) represents the values of the yield tensile strength of CFRP strips, respectively. This part of the study attempts to predict the propagation of the tensile force curve acting on CFRP strips and the tensile force equation used is adapted from reference [4] and written in Eq's. (6) and (7).

$$T_s \;= \begin{cases} 0 & if\ V \le V_C \\ \omega(V - V_C) & if\ V > V_C \end{cases} \tag{6}$$

$$\omega = \frac{2.5}{N_s \rho_s} \tag{7}$$

Equation 7 is an empirical equation used on steel stirrups and can be used for reinforced concrete with a square cross-section. The specimens in this study are reinforced concrete with a circular cross-section, and CFRP strips are used to resist shear forces. The author believes it necessary to modify Equation 7 to obtain the tensile force behavior on CFR strips. The data from the test results were used in statistical analysis to obtain modifications of ω. Statistical analysis using the linear regression method has been carried out, and the new modified equation ω as shown in Eq. 8 is proposed, where ρ_f is the ratio of CFRP strips.

$$\omega\ modified = \frac{0.08}{\rho_f} \tag{8}$$

It is seen from Fig. 7 that Eq. 8 can predict the tensile force that occurs in the CFRP strip well. In addition, the predictions obtained from Eq. 8 are conservative enough to predict the tensile force in CFRP strips.

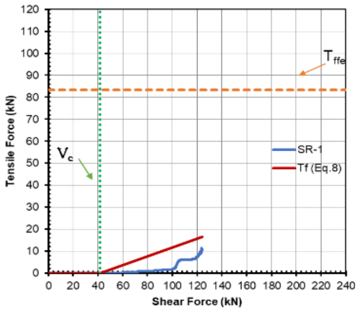

a) SR-1.

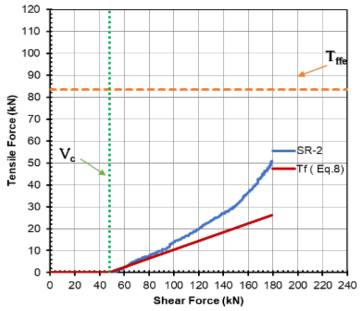

b) SR-2.

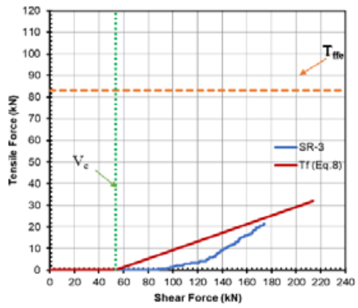

c) SR-3.

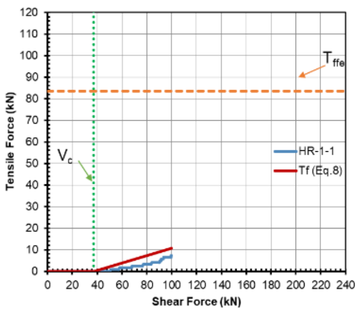

d) HR-1-1.

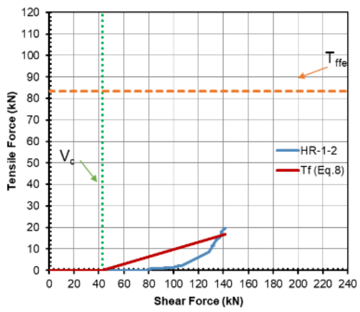

e) HR-1-2.

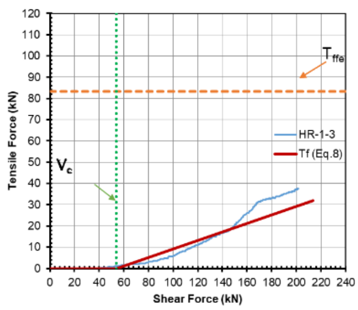

f) HR-1-3.

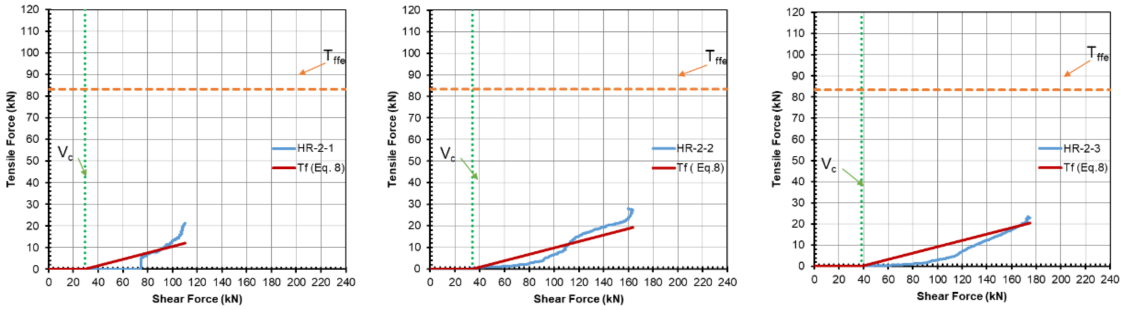

g) HR-2-1. h) HR-2-2. i) HR-2-3.

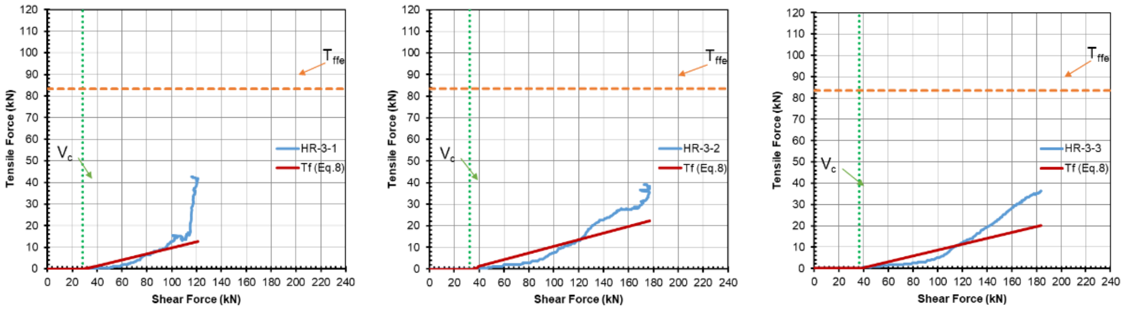

j) HR-3-1. k) HR-3-2. l) HR-3-3.

Fig. 7: Tensile forces on CFRP strips.

Comparison of the tensile force calculation results using the proposed formula with the test results provides an accuracy level of approximately 90% or a level of difference with the test results of around 10%. This result shows that the proposed formula provides quite good predictions.

6 Conclusion

Twelve specimens were tested and presented in this report. The tensile force behavior of CFRP strips has been analyzed, and an equation to calculate the tension force is proposed. The conclusions that can be drawn are as follows:

1) As expected, CFRP strips were proven to withstand shear forces well, with evidence of all flexural failure specimens showing indications of flexural tensile reinforcement yielding and crushing in the compressed concrete zone.

2) Analytical predictions with fiber element models show good predictions. However, there is a minor disagreement in the specimen with a higher ratio of longitudinal reinforcement owing to the higher intensity shear forces caused by the high flexural strength of the specimen.

3) The tensile force in the longitudinal reinforcement shows a significant increase in strain after the first crack occurs. However, the tensile force on CFRP strips increased significantly after diagonal cracking occurred in the specimen.

4) The equation used to predict the tensile force in CFRP strips shows values that differ by about 10% from the test results. However, the predictions obtained from this equation are conservative enough to predict the tensile forces in CFRP stirrups and strips.

Acknowledgment

The authors would like to express their gratitude to PT. Fyfe Fibrwrap Indonesia for providing CFRP material support. The authors thank the Faculty of Engineering, Andalas University, for funding research through Hibah Penelitian Unggulan in the financial year 2023.

References

[1] THAMRIN, R. - KAKU, T.: Bond behavior of CFRP bars in simply supported reinforced concrete beam with hanging region. Journal of Composites for Construction, ASCE, Vol. 11, č. 2, 2007, pp. 129-137.

[2] THAMRIN, R. - ZAIDIR. - HARIS, S.: Shear capacity of reinforced concrete beams strengthened with web-side bonded CFRP sheets. MATEC Web of Conferences, 2019.

[3] THAMRIN, R. - ZAIDIR. - DESHARMA, S.: Debonding Failure Analysis of Reinforced Concrete Beams Strengthened with CFRP Plates. Polymers MDPI, č. 13, 2021, pp. 1-20.
[4] THAMRIN, R.: Effect of end anchorage length and stirrups ratio on bond and shear capacity of concrete beams with nonmetallic reinforcement. Journal of Engineering Science and Technology, sv. 11, č. 6, 2016, pp. 768-787.
[5] CLARKE, J. L. - BIRJANDI, F. K.: The behaviour of reinforced concrete circular sections in shear. The Structural Engineer, sv. 71(5), 1993, p. 7378.
[6] THAMRIN, R. - KURNIAWAN, R. - MELINDA, A. P.: Shear and flexural capacity of reinforced concrete members with circular cross section. Procedia Engineering, 2017.
[7] HADI, M. N. S. - JAMEEL, M. T. - SHEIKH, M. N.: Behavior of circularized hollow RC columns under different loading conditions. Journal of Composites for Construction, sv. 5, č. 21, 2017.
[8] ALAJARMEH, O. - MANALO, A. A. - BENMOKRANE, B. - KARUNAS. - MENDIS, W. - NGUYEN, K.:Compressive behavior of axially loaded circular hollow concrete columns reinforced with GFRP bars and spirals. Construction and Building Materials, sv. 194, 2019, pp. 12-23.
[9] ALAJARMEH, O. S. -MANOLO, A. C. - BENMOKRANE, B. - KARUNASENA, K. - FERDOUS, W. - MENDIS, P.: Hollow concrete columns: Review of structural behavior and new designs using GFRP reinforcement. Engineering Structures, sv. 203, 2020, pp. 1-16.
[10] HOROWITZ, B.: Shear Strength of Hollow Circular Sections. IBRACON, sv. 9, 2016, pp. 214-225.
[11] DEWI, S. H. - THAMRIN, R. - ZAIDIR - TAUFIK.: Effect of stirrup type on shear capacity of reinforced concrete members with circular cross section. E3S Web Conf, sv. 156, 2020, pp. 4-7.
[12] THAMRIN, R. - TANJUNG, J. - ARYANTI, R. - NUR, O. F. - DEVINUS, A.: Shear strength of reinforced concrete T-Beams without stirrups. Journal of Engineering Science and Technology, sv. 11, č. 4, 2016, pp. 548-562.
[13] ALI, A. H. - MOHAMED, H. M. - BENMOKRANE, B.: Shear strength of circular concrete beams reinforced with GFRP bars. Resilient Infrastructure, London, 2016.
[14] FELTHAM, I.: Shear in reinforced concrete piles and circular columns. The Structural Engineer, sv. 84, č. 11, 2004, pp. 27-31.
[15] THAMRIN, R. - DEWI, S. H. - ASRIANUR, A. - YASTARI, F. P. - HARIS, S.: Shear Capacity of Hollow Reinforced Concrete Members without Stirrups. 5th ICEEDM, Yogyakarta, E3S Web Conf 2023.
[16] THAMRIN, R. - ZAIDIR. - HARIS, S. - DEWI, S. H. - YASTARI, F. P.: Shear capacity of hollow circular reinforced concrete members without stirrups strengthen with CFRP. Lectures Notes in Civil Engineering FIB Symposium, sv. 1, 2023, pp. 1217-1225.
[17] MEDHLOM, M. K. - ABED, E. N.: Behavior and Load Capacity of Concrete Slab Reinforced by CFRP Bar and Strengthening by CFRP Laminates. Civil and Enviromental Engineering, Vol. 19, č. 1, 2023, pp. 72-85.
[18] LIGNOLA, G. P. - PROTA, A. - MANFREDI, G. - COSENZA, E.: Performances of RC Square Hollow Columns Wrapped with CFRP under shear-type load. Challanges for civil construction, Porto, 2008.
[19] WANG, D. - HUANG, L. - YU, T.: Seismic performance of CFRP-Retrofitted Large-Scale square RC Columns with High Axial Compression Ratios. J. Compos. Constr, sv. 21, 2017.
[20] Guide for the Design and Construction of Externally Bonded FRP Systems for Strengthening Concrete Structures (ACI 440.2R-17). Farmington Hills: American Concrete Institute (ACI), 2017.
[21] KISHIDA, S.: Experimental Study On Shear Strength of The PHC Pile with Large Diameter. Journal of Structural and Construction Engineering. 1998, pp 123-130.
[22] THAMRIN, R.: Analytical prediction on flexural response of RC beams strengthened with steel plates. MATEC Web Conference, sv. 103, 2017, p. 2012.
[23] PARK, R. - PAULAY, T.: Reinforced Concrete Structure. New York: John Wiley, 1975.
[24] THAMRIN, R.: Effect of Strengthening Method and Development Length on Flexural Strength of RC Beams With Steel Plates. Journal of Engineering Science and Technology, sv. 13, č. 11, 2018, pp. 3781-3794.
[25] ZAIDIR. - THAMRIN, R. - DALMANTIAS, E.: Evaluation of the Pre-Cracked RC Beams Repaired with Sealant Injection Method, International Journal on Advanced Science Engineering Information Technology. sv. 7, č. 2, 2017, pp. 380-386.
[26] ACI Committee 318.: Building Code Requirements for Structural Concrete, ACI 318-19, Farmington Hills, American Concrete Institute., 2019.